International Research Journal of Engineering and Technology (IRJET) e-ISSN: 2395-0056
Volume: 02 Issue: 08 | Nov-2015 www.irjet.net p-ISSN: 2395-0072

One-Dimensional Optimization for Proportional–Resonant Controller Design along with fuzzy logic controller Against the Change in Solar Irradiation and Source Impedance in PV Systems

S.Thej Kiran[1], Y.VishnuVardhan Reddy[2]

[1]*PG Scholar, Department of EEE, JNTU Anantapuramu, Andhra Pradesh, India*
[2]*PG Scholar, Department of EEE, JNTU Anantapuramu, Andhra Pradesh, India*

Abstract - ***The changes in solar irradiation and source impedance impact on photovoltaic (PV) system control performance is examined. To acquire steady sinusoidal current tracking control for the grid-tied inverter, an internal-model-based undamped proportional resonant (PR) controller is employed for the PV inverter that would ease the control-loop design and improve the system performance. Proportional Resonant (PR) controller have advantages such as low-cost computational resources and spontaneous tracking capability. Despite the advantages of PR controller such as spontaneous tracking capability, the tracking performance may decrease due to sudden changes in solar irradiation and source impedance. So to accustom PR controllers over distinct operating conditions without acquiring redundant tracking error, an ODO algorithm is proposed to search the best χ with minimum steady state error. Therefore, the control gains of PR controller are updated for accommodating the VSI to the changed operating condition. The VSI is modulated using a Pulse Width Modulator according to the changed operating conditions. Fuzzy logic controller and proportional integral controller are used in the DC voltage regulator. FLC generates the required small change for voltage to control the magnitude of the injected voltage. Sinusoidal tracking is even more accurate with the addition of fuzzy controller into the system. The simulation is analyzed and carried out by using SIMULINK/MATLAB software for various values of χ.***

Key Words: *Proportional–resonant (PR) controller, voltage sourced inverter (VSI).*

1. INTRODUCTION

The interest in renewable energy sources has been increased with the high dependence of global economies on fossil fuels. Solar power is becoming more cost competitive because it is an inexhaustible source, maintenance free and available all over the world. Among the diverse solar power generation technologies, the grid-connected photovoltaic (PV) system has experienced potential growth due to the programs supported by governments and utility companies [1]. Inappropriate PV system control will result in negative impacts on power quality [2]–[4].

Synchronous *d*–*q* coordinate transformation offers a PV inverter with a useful solution for the decoupled control of active and reactive power. This would give rise to the coupling between *d*- and *q*-axis currents. Decoupled control of *d*- and *q*-axis currents has been proposed to condition the output power of a PV inverter [5]–[7]. A stationary frame current control with simple and less computation compared with the synchronous frame method has become another choice [8] to completely decouple PV inverter d- and q- axis currents. The proportional–integral (PI) controller can provide large gain for dc signal attributed to a pole at the origin. But utilizing the PI controller for sinusoidal current tracking control in a stationary frame would be a problem because the control gain at grid frequency is limited. So to achieve tight sinusoidal current tracking control for the grid-tied inverter, an internal-model-based proportional–resonant (PR) controller with large gain at the grid frequency would ease the control-loop design and improve the system performance.

This paper presents a One-dimensional optimization (ODO) algorithm that provides the PR controller with tight current tracking for the grid-tied PV inverter. The PR controller is a self tuning controller which can adapt to system uncertainty without complex computations and analysis. The contents of this paper are as follows. First, the system configuration with a single-phase PV inverter is described. The dynamic equations for the PV inverter are then derived from fig.1 and analyzed. Next For providing the controller with time reference and to realize the transformation between *d*-*q* axes and *α*–*β* axes a software phase locked loop is utilized. By using the ODO algorithm a self tuning PR controller for the grid tied PV inverter is then designed. Then the role of Fuzzy Controller in controlling the magnitude of injected

voltage is discussed. Finally simulation results arepresented along with important points in the conclusion.

2. SYSTEM CONFIGURATION AND CONTROL DESIGN OF SINGLE-PHASE PV INVERTER

The circuit configuration for a single-phase inverter is shown in Fig.1 in which four power switches (S1–S4) are used to modulate the dc voltage into ac form for coupling the grid utility. The phase of the point of common coupling (PCC) voltage v is used as a time reference for the inverter output voltagemodulation. So to express an instantaneous sinusoidal function ($v_\alpha(t) = V_m\cos(\omega_o t+ \theta_{v0})$) as a vector that contains the phase angle and magnitude, a virtual orthogonal function $v\beta(t)$ which has the same magnitude as $v_\alpha(t)$ is created to act as the imaginary part of a vector **v** as follows:

$$\mathbf{v} = v_\alpha + jv_\beta \quad (1)$$

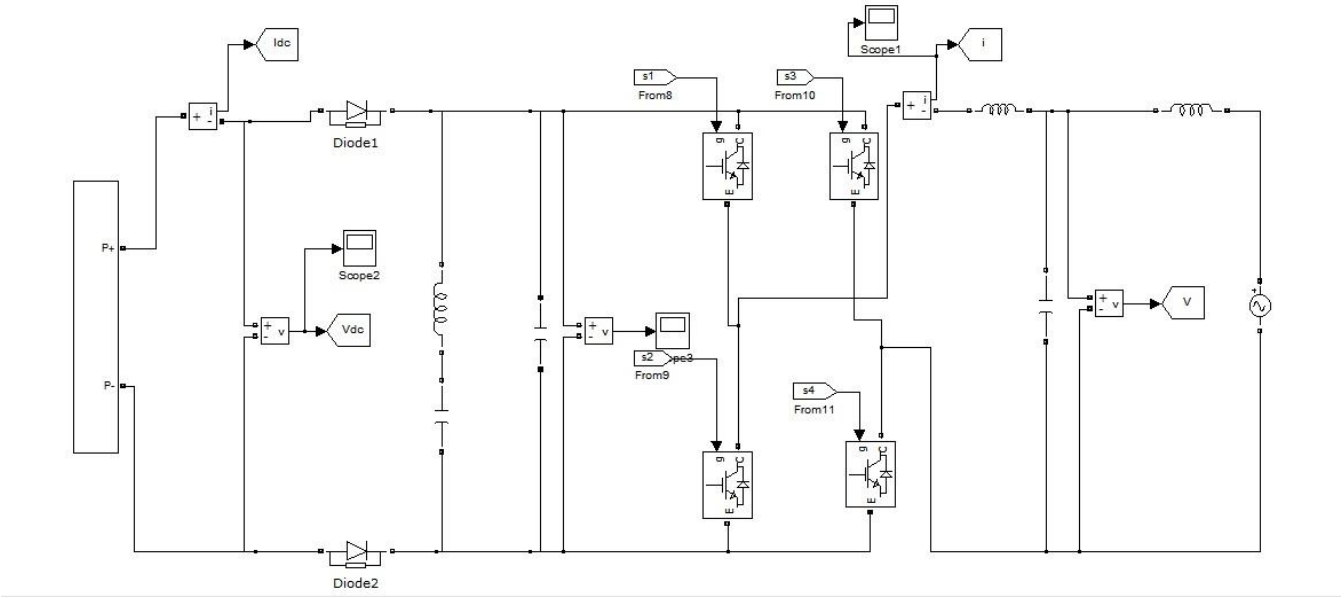

Fig-1:Simulink Diagram of System configuration for a single-phase grid-tied PV inverter

The inverter can parallel with the grid accordingly when the absolute angle and magnitude of the PCC are obtained. By using KVL the model of the coupling filter between PCC bus and the inverter terminal is described in the vector form as follows:

$$L_x \frac{di}{dt} = -r_x \cdot i + (v_e - v) \quad (2)$$

whereL_x and r_x are the equivalent inductance and resistance of the coupling inductor respectively.

The vector representation in (2) can be resolved into real and imaginary parts in α–β axes in the following form:

$$L_x \begin{bmatrix} \frac{di_\alpha}{dt} \\ \frac{di_\beta}{dt} \end{bmatrix} = -\begin{bmatrix} r_x & 0 \\ 0 & r_x \end{bmatrix}\begin{bmatrix} i_\alpha \\ i_\beta \end{bmatrix} + \begin{bmatrix} v_{e\alpha} - v_\alpha \\ v_{e\beta} - v_\beta \end{bmatrix} \quad (3)$$

The instantaneous complex per-unit power through a coupling path to the VSI at the PCC bus can be represented as follows:

$$S = \mathbf{v} \cdot i^*$$
$$= (v_\alpha + jv_\beta)(i_\alpha - ji_\beta)$$
$$= (v_\alpha i_\alpha + v_\beta i_\beta) + j(v_\beta i_\alpha - v_\alpha i_\beta) \quad (4)$$

Active power P and reactive power Q can be derived as:

$$P = v_\alpha i_\alpha + v_\beta i_\beta \quad (5)$$

$$Q = v_\beta i_\alpha - v_\alpha i_\beta \quad (6)$$

Equation (3) shows that the current in α-β axes is independent to each other. Therefore it follows a direct rule that the current control in α-β axes (i_α,i_β) is achieved by changing the inverter output voltage in α- and β-axes ($v_{e\alpha}$,$v_{e\beta}$), respectively. (5) and (6) describes the facts that the active and reactive power values are coupled with the inverter output current in both α-β axes. A synchronous reference frame (d–q axes), is defined where the d-axis is always coincident with the instantaneous PCC bus voltage vector **v** and the q-axis is in quadrature with it. The d-axis component is entirely

the magnitude of the voltage vector and the projection of the voltage vector **v** onto the *q*-axis would be zero.

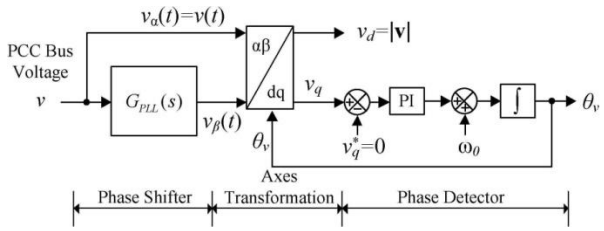

Fig-2: Block diagram of the SPLL

Therefore,

$$P = v_d i_d \quad (7)$$
$$Q = -v_d i_q \quad (8)$$

In (7) and (8) the *d*-axis current component $i_d$is the instantaneous active power and the *q*-axiscurrent component $i_q$is the instantaneous reactive current.

The angle $\theta_v$between vector **v** and the α-axis in Fig.2 can be obtained by two steps. The first step is to let $v_\alpha(t) = v(t)$ and make up a virtual orthogonal function $v_\beta(t)$ using the below transformation.

$$v_\beta = G_{PLL}(s) v_\alpha \quad (9)$$

$$G_{PLL}(s) = \frac{w-s}{w+s} \quad (10)$$

The transfer function $G_{PLL}(s)$ in (10) is an all-pass filter. It can provide 90phase lags withoutattenuating the magnitude in $v_\beta(t)$.. Fig. 3 assimilates the two steps that are advantageous in providing a grid-tied inverter with the time reference for decoupling the power control and paralleling.

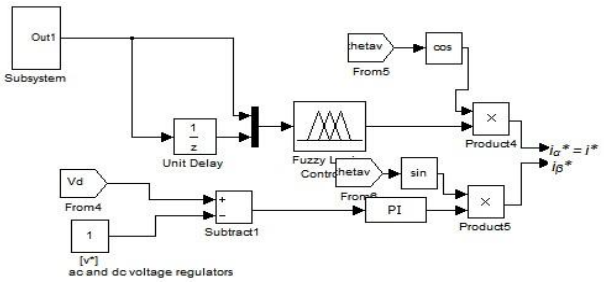

Fig-3:Block diagram of the ac and dc voltage regulators

As shown in Fig.3 the active power control for the grid-tied PV inverter was carried out by a dc voltage regulator. Here the voltage command v^*_{dc} is determined by a maximum power point tracking (MPPT) algorithm. An ac bus voltage regulator was performed using reactive power compensation to improve the voltage quality for the PCC bus under distinct PV power generation conditions. By summing up the projection of the current components on the α-axis contributed by i^*_d and i^*_q we can obtain the current command i_α.

2.1 Proportional Resonant Controller

PI controller provides large gain for the dc signal attributed to a pole at the origin. Therefore it is quite appropriate for the voltage magnitude control, as shown in Fig. 3. When using the PI controller, the sinusoidal current tracking control in α-β axes would be a problem because the control gain at the grid frequency is limited. So to accomplish tight sinusoidal current tracking, a controller with large gain at the grid frequency would improve the system performance

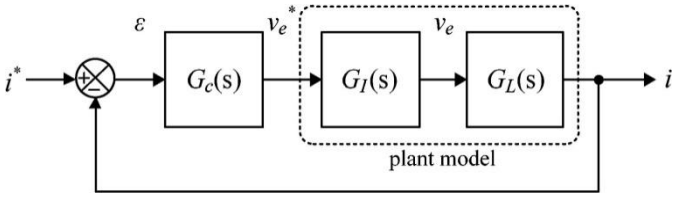

Fig-4: Block diagram of the current control system

In the above fig.4 $G_C(s)$, $G_I(s)$, $G_L(s)$ and are the models of the controller, inverter, and coupling filter, respectively.

The error function $E(s) = L\{\varepsilon(t)\}$ for a sinusoidal input of magnitude A can be expressed as

$$E(s) = \frac{1}{1+G_c(s)G_I(s)G_L(s)} \frac{A\omega_o}{s^2+\omega_o^2} \quad (11)$$

$D(s)$ contains a quadratic factor in the following form:

$$D(s) = (s^2 + \omega_o^2) D_o(s) \quad (12)$$

The PR controller is given by

$$G_c(s) = K_p + \frac{bs}{s^2+as+\omega_o^2} \quad (13)$$

where$K_p$is the proportional gain, b is the resonant gain, and a relates to the damping of the controller. As shown in (12), with a=0 PR controller is characterized by excellent steady-state tracking performance.
The closed-loop transfer function of the current control system is

$$\frac{I(s)}{I^*(s)} = \frac{G_c(s)G_I(s)G_L(s)}{1+G_c(s)G_I(s)G_L(s)} \quad (14)$$

A simple R–L circuit model (as shown in Fig. 1) is used to simulate the series coupling inductor.

$$G_L(s) = \frac{1}{sL_x+r_x} \quad (15)$$

Substituting (13) and (16) in (14) gives a characteristic

equation

$$S^3 + \frac{(L_x a + r_x + k_p)}{L_x} S^2 + \frac{(\omega_o^2 L_x + r_x a + k_p a + b)}{L_x} S + \frac{(r_x + k_p)\omega_o^2}{L_x} = 0 \quad (16)$$

To obtain satisfactory system performance, a pole assignment method was employed by selecting a pair of conjugate poles and a real pole in the desired characteristic equation

$$(s + \chi\zeta\omega_n)(s^2 + 2\zeta\omega_n s + \omega_n^2) = 0 \quad (17)$$

whereω_n, χ and ζ are selected to meet the design specifications, a non-dominant root is defined by$s + \chi\zeta\omega_n = 0$ and the roots of $s^2 + 2\zeta\omega_n s + \omega_n^2 = 0$ are the dominant roots.
The above equation can be expanded as

$$S^3 + (\chi\zeta\omega_n + 2\zeta\omega_n)S^2 + (2\chi\zeta^2\omega_n^2 s + \omega_n^2)S + \chi\zeta\omega_n^3 = 0 \quad (18)$$

Comparing (16) and (18),

$$K_p = \frac{\chi\zeta\omega_n^3 L_x}{\omega_o^2} - r_x \quad (19)$$

$$a = \zeta\omega_n(\chi + 2) - \frac{r_x + K_p}{L_x} \quad (20)$$

$$b = \omega_n^2(2\chi\zeta^2 + 1)L_x - \omega_o^2 L_x - a(r_x + K_p) \quad (21)$$

The damping ratio of the resonant controller (13) should be maintained at zero (a = 0), to eliminate the steady state error. By substituting (20) into (21), we get

$$\omega_n = \omega_o\sqrt{\frac{2+\chi}{\chi}} \quad (22)$$

When compared with the damped PR controller (a = 200) the undamped PR controller(a = 0) decreases the steady-state error of the current response. Equations (20)–(23) also show a direct rule to determine the control gains for the undamped PR controller when relevantχ is chosen.

For evaluating the natural frequency ω_n effect on the steady state error, an evaluation function *ISE* defined as the integral of the square of the error (ISE) is given by

$$ISE = \int_0^\infty \varepsilon^2(t)dt = \int_0^\infty [i^*(t) - i(t)]^2 dt \quad (23)$$

High damping ratio would cause higher control gain values, which is more advantageous to reducing the ISE. The increase in control gains results in decrease in system's immunity from noise and model uncertainty. To constrain the control gains and to guarantee the low ISE for dampening the current tracking error, χ should be greater than 10. A pilot calculation for ISE and control gains is provided in [9]Table I.

2.2 ODO for Searching Control Gain with Minimal Steady- State Error

An ODO algorithm is proposed to search the best χ with minimum steady-state error, to adapt the VSI controller over diverse operating points along with satisfactory performance. In this procedure, the ISE plays a main role on changing the searching direction for χ.Therefore when there is a change in operating condition the control gains for the voltage source inverter (VSI) can be updated as shown in Fig.4.

When there is a suggestive change in the operating point, the current tracking error can be detected by the ODO to update the control gains for indulging the VSI to the changed operating points. The procedures followed by the proposed ODO algorithm to adjust the Proportional Resonant (PR) controller are:

(1) *Sum up the current tracking error:* In designing the self-tuning PR controller for the VSI, it is essential for the system to provide an effective index for measuring the control performance for the ODO to update the control gains k_p,b,ω_n. The ISE criterion provided by (23) is used to collect current tracking performance.

(2) *Correct the control direction*: When the latest $ISE_n$is greater than the prior ISE_{n-1}(ΔISE >0), for minimizing the current tracking error thecontrol direction of χ is changed in the reverse direction.

(3) *Update the control gains*: When the control direction for χ is changed, the control gains k_p,b,ω_n are updated according to the equations (19), (21), and (22).

START

A

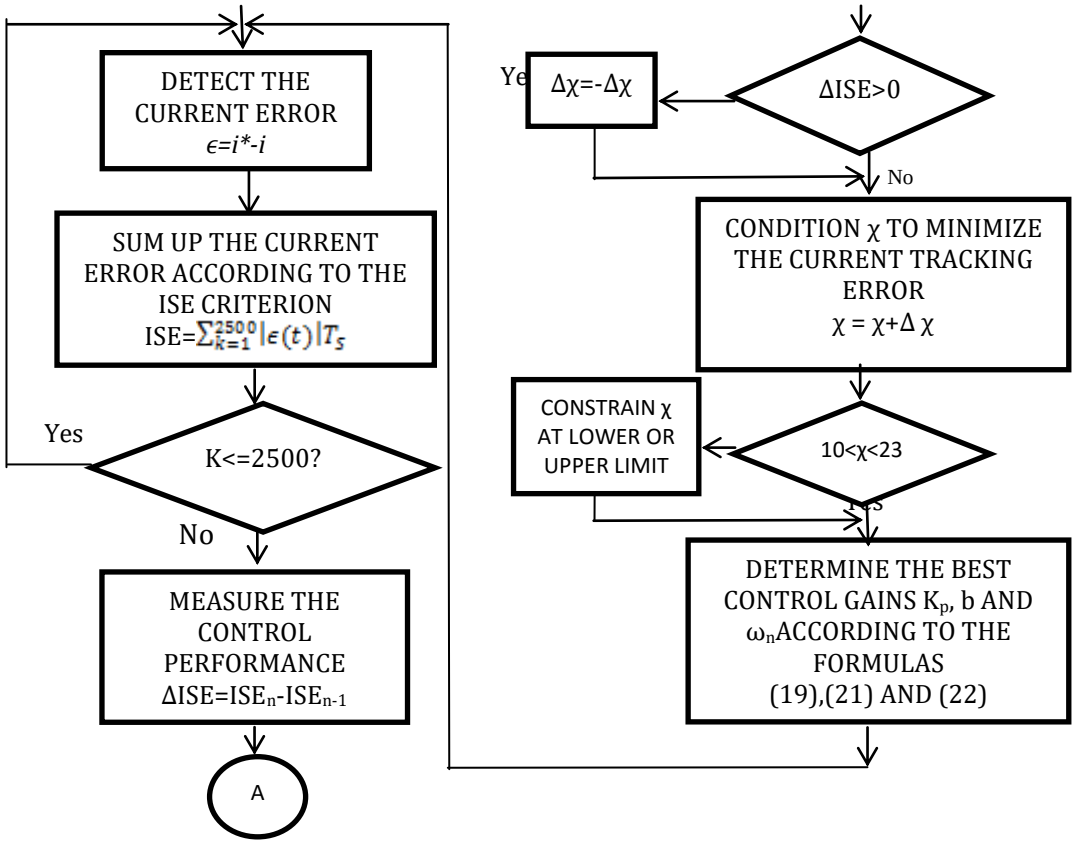

Fig-5: Flowchart for the procedure of adjusting χ by the proposed ODO.

3. FUZZY LOGIC CONTROLLER

To assure the effective performance of controller over wide range of system operations and to increase the transient stability of the system, a supplementary fuzzy logic controller (FLC) based on the Mamdani's fuzzy inference method is designed. The centroid defuzzification technique is used is this fuzzy controller.

The below fig describes the FLC structure. In this case, a two–input, one–output FLC is considered. The Fuzzy Controller is replaced with PI controller in DC voltage regulator block. The input signals are voltage error andrate of change of voltage error and the resultant output signal is the current. By employing Fuzzy Controller the ripples are reduced to a great extent even when the χ value is selected above 23.Sinusoidal tracking is even more accurate with the addition of fuzzy controller into the system.

There are two linguistic variable for each input variable, including, “Positive” (P), and “Negative” (N). For the output variable there are three linguistic variables, namely, “Positive” (P), “Zero” (Z) and “Negative” (N).

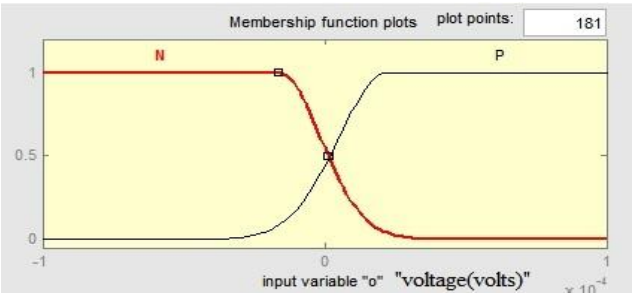

Fig-(8a): Membership function of input 1 (error voltage)

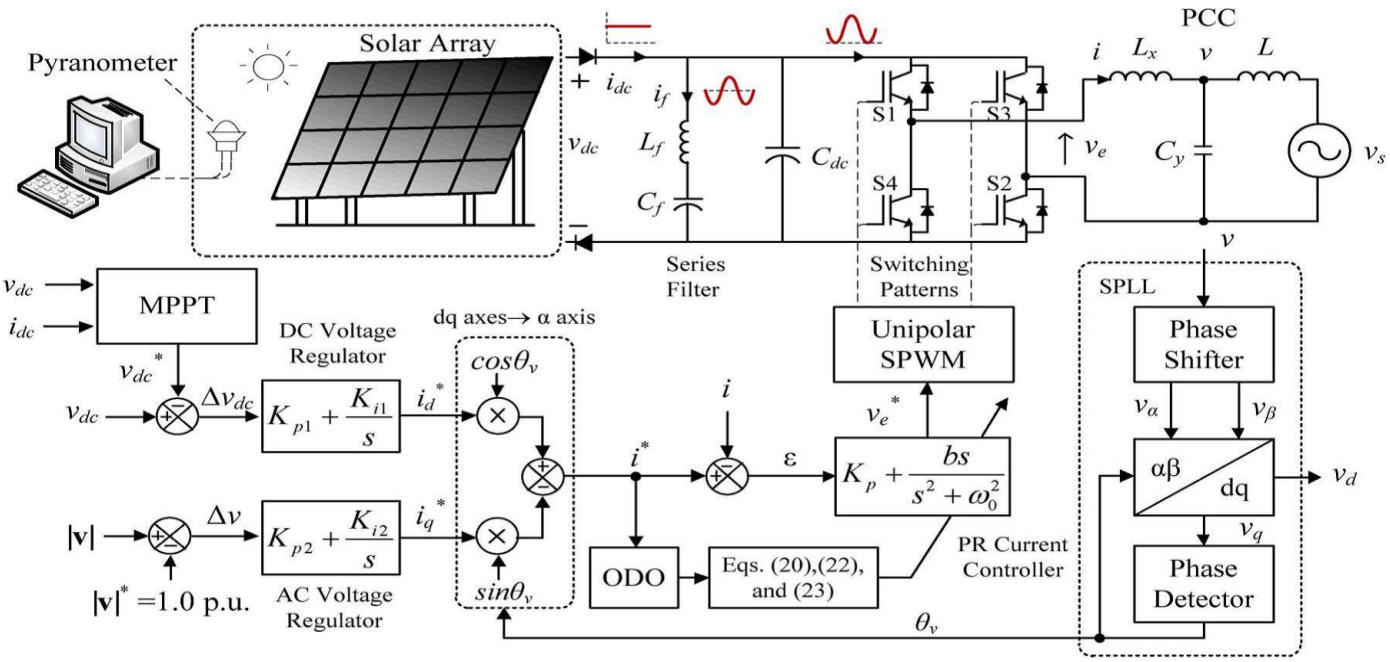

Fig-6: Schematic diagram

TABLE-1: CIRCUIT PARAMETERS

Power Grid (60Hz)		
source impedance	L / r	10mH/ 0.86Ω
PV array (1.5kW)		
rated open circuit voltage		561.6V
rated short circuit current		3.55 A
rated irradiation		1000W/m^2
Inverter Rating 3kVA		
coupling filter (at 60Hz)	L_x/r_x	5.15mH/58m Ω
dc-link capacitance	C_{dc}	2350μF
shunt capacitance (A conn.)	C_y	5μF
resonant LC filter	L_f/C_f	3.5mH/ 500μf
switching frequency	f_{sw}	15kHz (=1/T_s)
time delay	T_d	2.3 T_s
Control Gains		
ac voltage regulator	K_{p1},/K_{i1}	0.1/1
dc voltage regulator	K_{p2}/K_{i2}	0.1/1

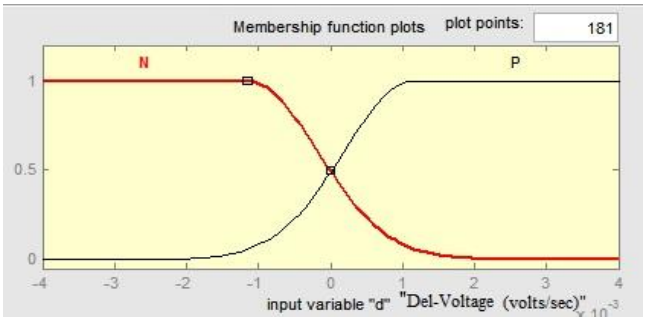

Fig-(8b): Membership function of input 2 (rate of change in error voltage)

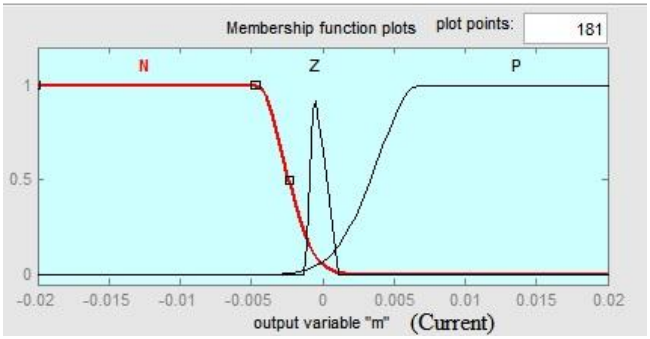

Fig-(8c): Membership function of output (current)

The rules used for the FLC are chosen as follows:
If o is P **and** d is P, **then** *m* is P.
If o is P **and** d is N, **then** *m* is Z.
If o is N **and** d is P, **then** *m* is Z.
If o is N **and** d is N, **then** *m* is N.

4. SIMULATION RESULTS AND DISCUSSION

The first two tests are used for verifying whether the condition of χ is efficient to accommodate the inverter to different operating conditions. The last two tests confirmed that the proposed voltage regulator is possible to achieve tight regulation in the PCC bus voltage.

4.1(Test 1) Adapt System Damping to Source Impedance

When source impedance changes in a PV system, the PCC bus voltage will not be constant and is inclined to disturbance, which not only intrudes with SPLL performance but also decays the current response. When two response curves between Figs 9 and 10 are compared it shows that the PCC bus voltage quality would be decayed due to the oscillatory current response when χ was selected over the upper bound of robust stability (χ = 23). The oscillatory current response can be dampened by choosing different χ's in case of the uncertainty in source impedance, which strengthens the importance of the ODO scheme for improving the voltage and current quality in PV systems.

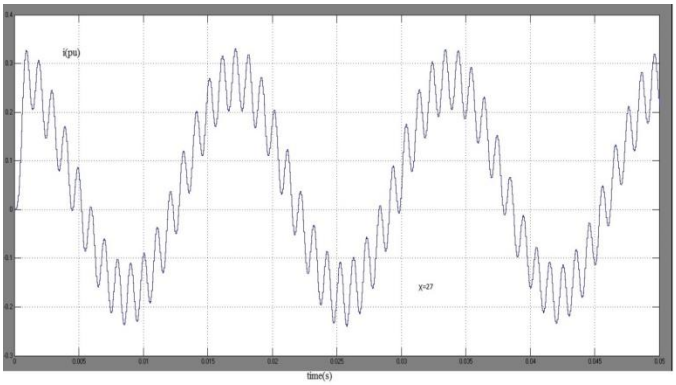

Fig-9(a):System responses of Test 1(L=0.0mH,v_{dc} =450V, i^*=0.333 pu) when χ=*27*(K_p= 3.2516,b = 2134.7)

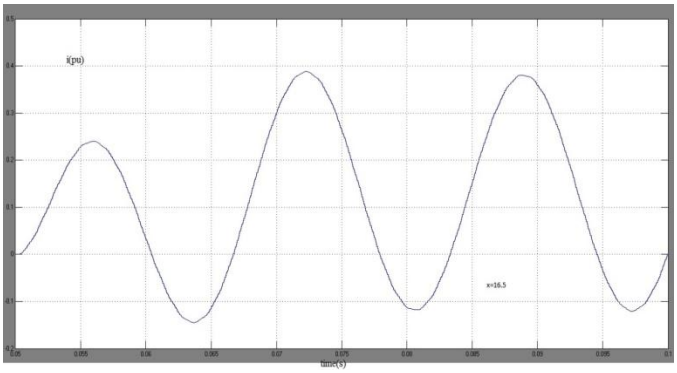

Fig-9(b):System responses of Test 1(L =0.0mH,v_{dc}= 450V, i^*=0.333 pu) when χ=*16.5*(K_p=2.1180, b= 1365.2)

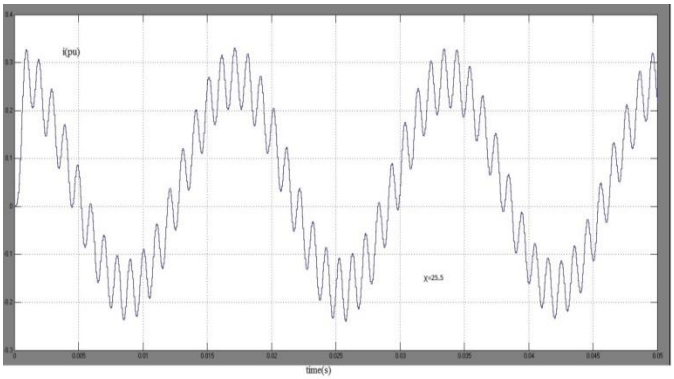

Fig-10(a):System responses of Test1(L=0.0mH,v_{dc}=450V, i^*=0.333pu)when χ=*25.5*(K_p=3.0894, b =2024.7)

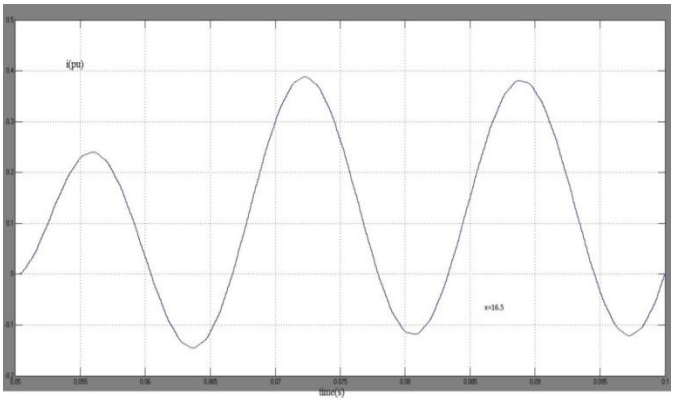

Fig-10(b):System responses of Test 1(L=0.0mH,v_{dc} =450V, i^*=0.333 pu) when χ=16(Kp= 2.0642, b = 1328.6)

4.2 (Test 2) Adapt System Damping to Solar Irradiation

When solar irradiation increases, the PV array would equip the PV inverter with more voltage.The output current of the PV inverter should be increased to acquire more power from the PV array. To relieve the tracking error for the high-irradiation case, a high value of χ compared to Test 1 should be taken up. The best method to decrease the current deviation is to alter χ to decline the control gains to adapt PV inverter to the changed solar irradiation. Theconsequence of altering χ to the changed solar irradiation is shown in Figs. 11 and 12, which confirms that χ has prominent influence on the current response.

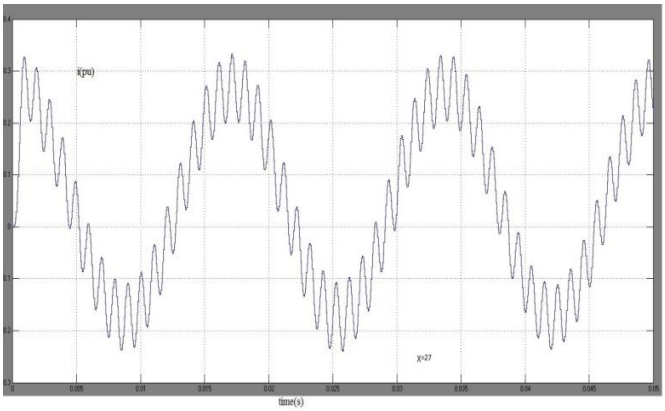

Fig-11(a):System responses of Test 2(L =0.0mH,v_{dc} =550V,i^*=0.5 pu) when χ = 27,K_p=3.2516,b = 2134.7)

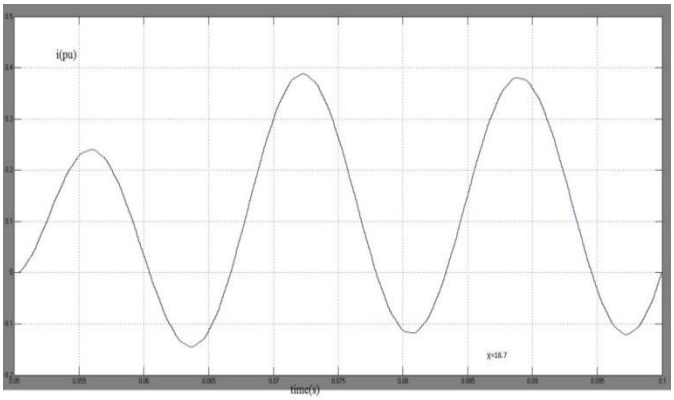

Fig-11(b):System responses of Test 2(L=0.0mH,v_{dc}=550V, i^*= 0.5pu)when χ=18.7(Kp=2.3552, b = 1526.2)

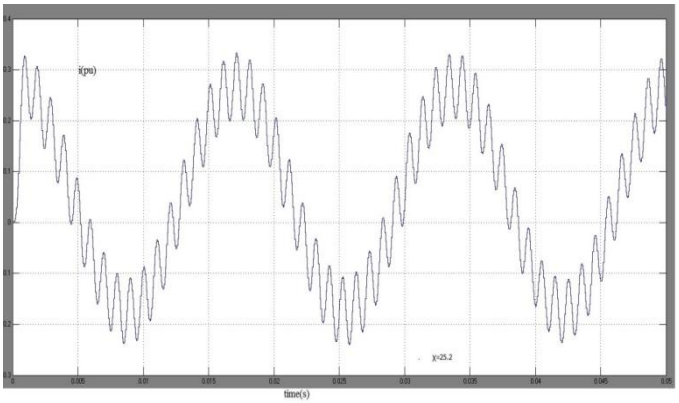

Fig-12(a): System responses of Test2(L=10.0mH,v_{dc}= 550V, i^*= 0.5 pu) when χ = 25.2(K_p=3.0894, b = 2024.7)

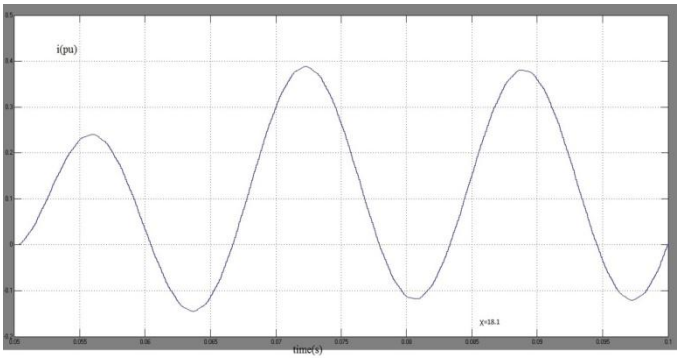

Fig-12(b): System responses of Test2(L=10.0mH,v_{dc}= 550V, i^*= 0.5 pu) when χ = 18.1(K_p=2.2905, b = 1482.3)

4.3 (Test 3) PCC Voltage Regulation

To accommodate control gains to distinct operating conditions for the PV inverter, the proposed controller is also capable of improving the PCC bus voltage quality using reactive compensation when the PV inverter is tied to the PCC bus. The output active power P_{dc} is consistent with the time-varying solar irradiation when the MPPT controller comes into play. The active power at dc-link voltage is then transferred to the power grid through the

proposed PR current controller. The proposed PR current controller accompanies the voltage regulator to acquire tight regulation in current response and also to assuage voltage fluctuation for the grid-tied PV inverter

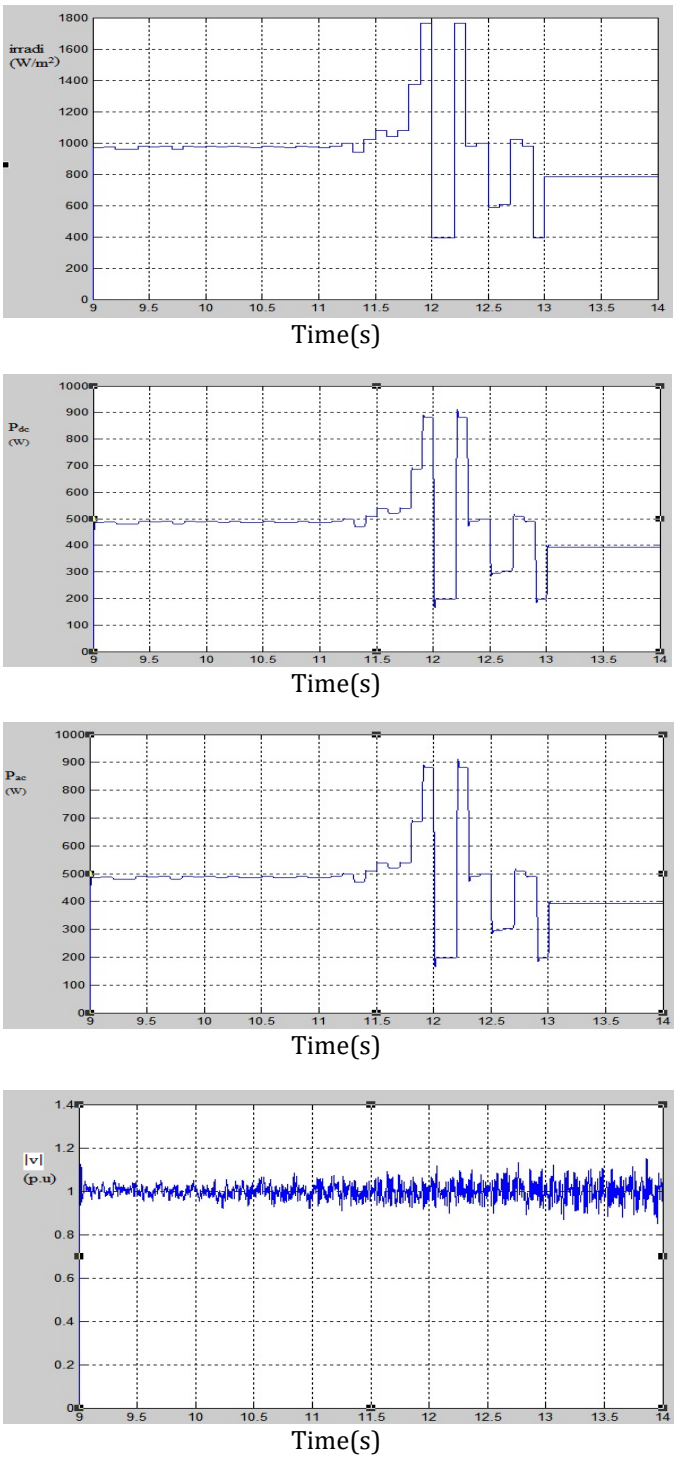

Fig-13: System responses without an ac voltage regulator

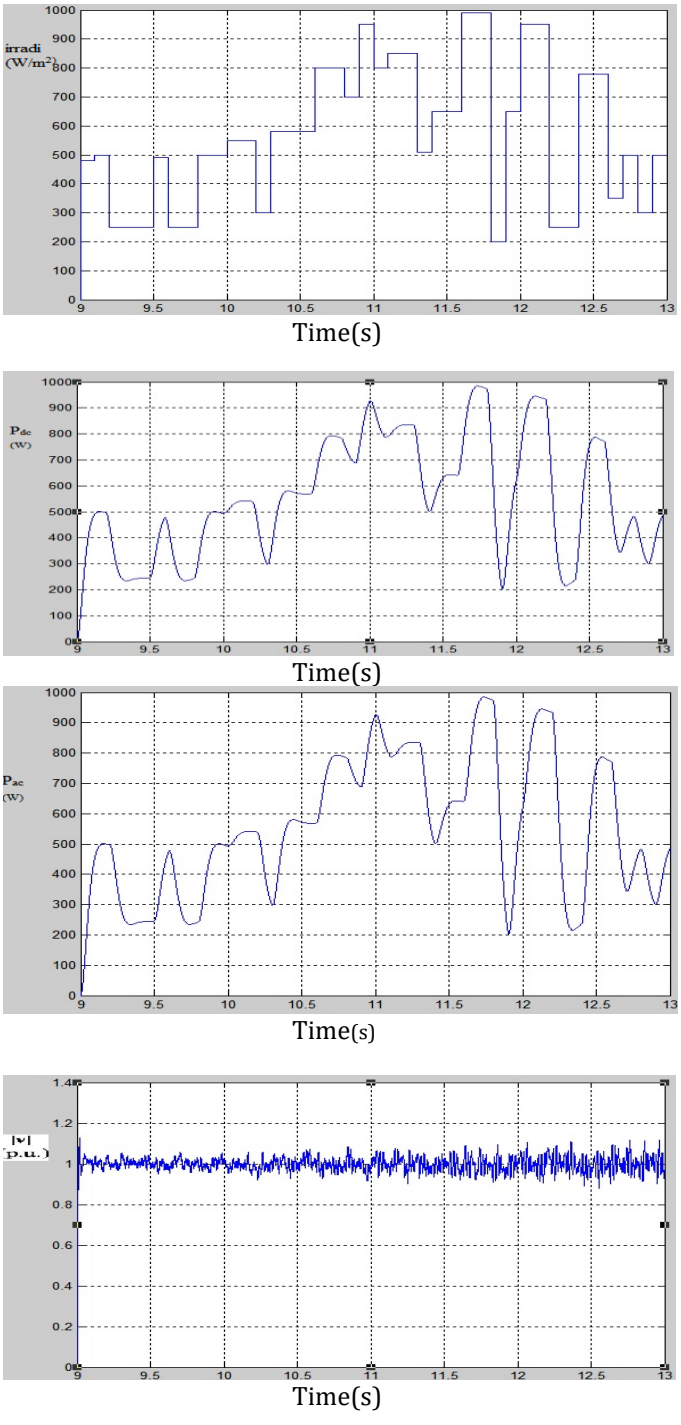

Fig-14: System responses with an ac voltage regulator.

5. CONCLUSION

An ODO-based PR current controller has been presented to adjust the grid-tied PV inverter to variations in solar irradiation and source impedance. To achieve instantaneous current control an undamped PR controller is employed for the PV inverter. The undamped PR controller is free from steady-state error

and has a larger bandwidth compared to the conventional damped PR controller. To change the control gains for minimal tracking error in current response the ODO adaptation scheme searches for a desired factor χ between the real part of the dominant and non-dominant eigen values. A voltage regulator is performed to handle dynamic system conditions to further improve PCC voltage quality for thegrid-tied PV inverter over distinct operating condition.By employing Fuzzy Controller the ripples are reduced to a great extent even when the χ value is selected above 23. Sinusoidal tracking is even more accurate with the addition of fuzzy controller into the system. The simulation results with the proposed theory show that the without incurring negative impacts in current and voltage responses the PV inverter can be interfaced to the distribution system and ride over the successive transients.

REFERENCES

[1] F. Blaabjerg, R. Teodorescu, M. Liserre, and A. V. Timbus, "Overview of control and grid synchronization for distributed power generation systems," *IEEE Trans. Ind. Electron.*, vol. 53, no. 5, pp. 1398–1409, Oct. 2006.

[2] Y. W. Li, D. MahindaVilathgamuwa, F. Blaabjerg, and P. C. Loh, "A robust control scheme for medium-voltage-level DVR implementation," *IEEE Trans. Ind. Electron.*, vol. 54, no. 4, pp. 2249–2261, Aug. 2007.

[3] M. Liserre, R. Teodorescu, and F. Blaabjerg, "Stability of photovoltaic and wind turbine grid-connected inverters for a large set of grid impedance values," *IEEE Trans. on Power Electronics*, vol. 21, no. 1, pp. 263–272, Jan. 2006.

[4] H. Liu and Y. Y. Hsu, "Design of a self-tuning PI controller for a STATCOM using particle swarm optimization," *IEEE Trans. Ind. Elec-tron.*, vol. 57, no. 2, pp. 702–715, Feb. 2010.

[5] W. L. Chen, W. G. Liang, and H. S. Gau, "Design of a mode decoupling STATCOM for voltage control of wind-driven induction generator sys-tems," *IEEE Trans. Power Del.*, vol. 25, no. 3, pp. 1758–1767, Jul. 2010.

[6] S. Fukuda and R. Imamura, "Application of a sinusoidal internal model to current control of three-phase utility-interface converters," *IEEE Trans.Ind. Electron.*, vol. 52, no. 2, pp. 420–426, Apr. 2005.

[7] N. Zmood and D. G. Holmes, "Stationary frame current regulation of PWM inverters with zero steady-state error," *IEEE Trans. Power Electron.*, vol. 18, no. 3, pp. 814–822, May 2003.

[8] H. Cha, T. K. Vu, and J. E. Kim, "Design and control of proportional–resonant controller based photovoltaic power conditioning system," in *Proc. IEEE Energy Convers. Congr. Expo.*, 2009, pp. 2198–2205.

[9] Woei-Luen Chen and Jhe-Shuan Lin, "One-Dimensional Optimization for Proportional–Resonant Controller Design Against the Change in Source Impedance and Solar Irradiation in PV Systems," *IEEE Trans. Ind. Elec-tron,* vol. 61, no.4,Apr. 2014.

BIOGRAPHIES

S.ThejKiran currently pursuingM-Tech in Control Systems at JNTUA College of Engineering and Technology Anantapur, Andhra Pradesh. His area of interest is Control Systems.

Y.VishnuVardhan Reddy currently pursuing M-Tech in Control Systems at JNTUA College of Engineering and Technology Anantapur, Andhra Pradesh.His area of interest is ControlSystems.